Experiment Study on Optimization of Electric Field Performance for Electrostatic Precipitator by Using Finite Element Method

DANG Xiaoqing, LI Dongyang, MA Guangda, REN Yan, SHI Yong
(School of Environmental & Municipal Engineering,
Xi'an University of Architecture & Technology, Xi'an 710055, PR China)

Abstract: The current density on the collecting plates were measured of 12 kinds of common discharge electrodes matched C480 and ZT24 collecting plates. The effect of different discharge electrodes and setting manners on the experiment results was discussed with two parameters of average current density and relative standard deviation. The distributions of electric potential and electric field strength were calculated by using finite element method when V serial discharge electrodes matched ZT24 collecting plates .Combining the results of the experiments and numerical calculation, the paper analyzed the effect of electric field strength on the corona current.

Keywords: Electrostatic precipitator; Distribution of current density; Average current density; Electric field strength; Finite element

1 INTRODUCTION

The collection efficiency of fine particle could be increased through enhancing the charges of particle and optimizing the characteristic of electric field. The corona power could be increased by enhancing corona current. The performance of electrostatic precipitator (ESP) is restricted by the current density and the electric strength near collecting plates. $E = j \cdot \rho$, where, E is the electric field strength of dust cell, j is the average current density of collecting plates, ρ is the specific resistance of particle. References indicate that if the distribution of corona current density is not uniform, it usually causes back corona and the average current density on the collecting plates is $1/10$[1-8] of the value calculated based on the breakdown field strength and dust in the deposit with specific resistance. Therefore, the corona current density and electric field strength are important indexes reflection of the performance of ESP.

2 EXPERIMENT DEVICE AND TESTING RESULTS

2.1 Experiment Device

The author built the experiment facilities with 12 kinds of discharge electrodes and the C480, ZT24 plates as the collector. The discharge electrode was 1 meter in length and 6 collecting plates (C480, ZT24) were arranged in two rows. A total of 25 probes were fixed in a horizontal line on a plate. The horizontal spacing between two probes was 10 mm. The plate provided with probes was movable vertically, the moving range of which was 150 mm by means of screw. The testing system included Tassicker probes, sampling switch box, bias power supply and ammeter and so on. The discharge electrodes and testing system were shown in Fig. 1 and Fig. 2 respectively. The distance between neighboring discharge electrodes were set according to the criterion of C480 collecting plate.

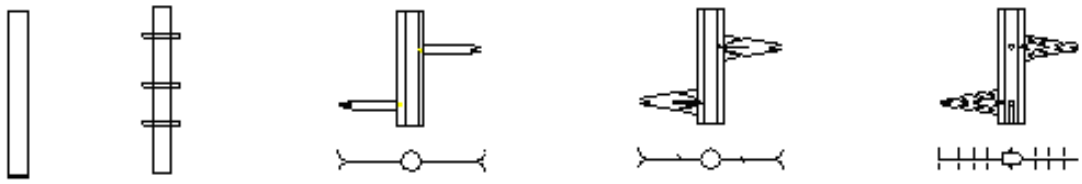

V discharge electrode RS discharge electrode Improved RS discharge electrode Ten bars discharge electrode

Fig. 1 Common discharge electrodes

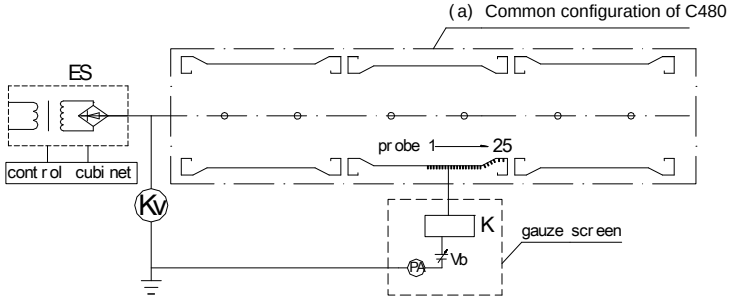

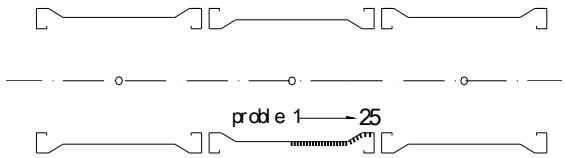

(b) sketch of electrode configuration(RS matched C480)

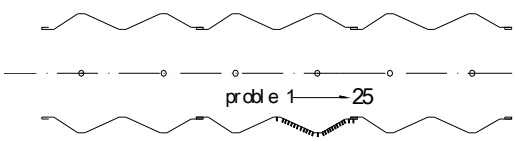

(c) sketch of electrode configuration(V matched ZT24)

Fig. 2 Test system of the experiments

2.2 Testing Results and Analysis

Under different electrode configurations, the average current density $\bar{j}$ and the standard variation of current density σ were used to evaluate the performance of the electric field.

$$\bar{j} = \frac{1}{n}\sum_{i=1}^{n} j_i \tag{1}$$

$$\sigma = \sqrt{\frac{1}{n}\sum_{i=1}^{n}\frac{(j_i - \bar{j})^2}{\bar{j}^2}} \tag{2}$$

where, n was the number of measuring points, j_i was the current density of measuring point i, mA/m^2.

Tassicker boundary probe[9] was used to measure the distribution of current density on the collecting plates. The spacing between two rows of collecting plates were selected 350 mm, 400 mm and 450mm. In the experiments, the operating voltage was adjusted to about 85% of the spark voltage. At different electrode configurations, the current density on the collecting plate was measured and the averages and the relative standard variation were calculated , which were shown in Table 1 and Figs. 3-5. From Table 1 it could be seen that on the condition of the same average electric field strength and spacing between two rows, current density of the surface of C480 was bigger than that of ZT24 collecting plates. When the plate spacing was 350 mm, the discharge electrodes RS, V15, V25,V40 had the biggest corona current ,while V0 had the biggest one at 400 mm. When the spacing between two rows of collecting plates were 400 mm, the relative standard variation of plate current densities were the best for RS, V15, V25, V40 electrodes, while V0 had the best one at 350 mm. When RS matched C480 and the plate spacing was 400mm, the average corona current were the biggest and the distribution of current density were better.

Table 1 Test results of current density

Experiment condition	Spacing 350 mm		Spacing 400 mm		Spacing 450 mm	
$\bar{E}$ =3.15 kV/cm	$\bar{j}$ /(mA·cm^{-2})	σ	$\bar{j}$ /(mA·cm^{-2})	σ	$\bar{j}$ /(mA·cm^{-2})	σ
RS-C480	0.723	0.689	0.708	0.598	0.610	0.711
V0-ZT24	0.234	0.620	0.249	0.627	0.163	0.649
V15-ZT24	0.574	0.528	0.518	0.470	0.480	0.509
V25-ZT24	0.659	0.475	0.652	0.437	0.610	0.480
V40-ZT24	0.669	0.388	0.588	0.376	0.579	0.380

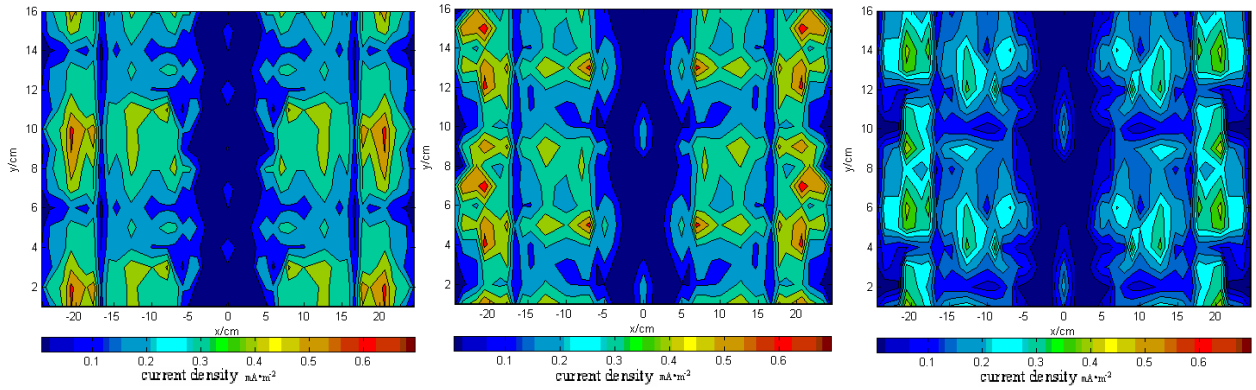

(a) Spacing 350 mm (b) Spacing 400 mm (c) Spacing 450 mm

Fig. 3 Distribution of current density(V0 matched ZT24)

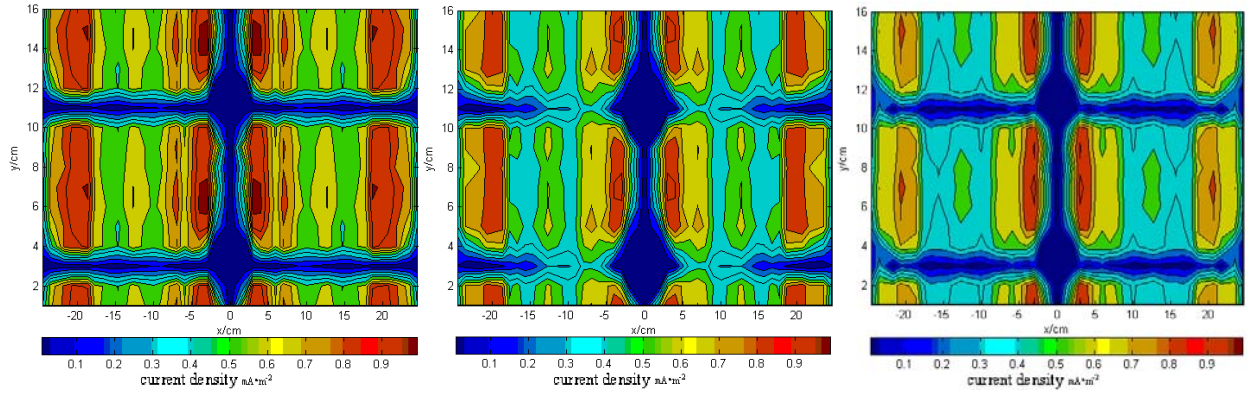

(a) Spacing 350 mm (b) Spacing 400 mm (c) Spacing 450 mm

Fig. 4 Distribution of current density(V15 matched ZT24)

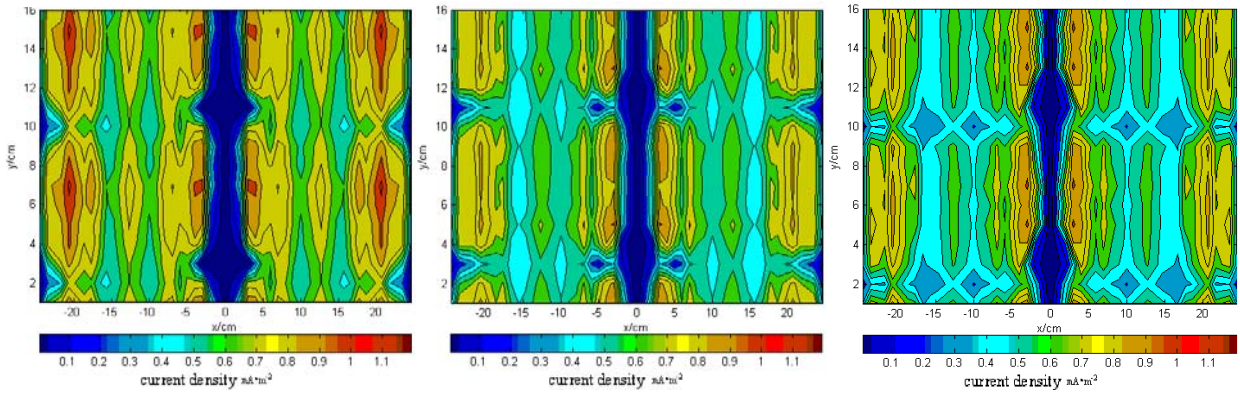

(a) Spacing 350 mm (b) Spacing 400 mm (c) Spacing 450 mm

Fig. 5 Distribution of current density(V40matched ZT24)

3 CALCULATION MODEL AND VALIDATION

3.1 Mathematic Model of Ion Field and Boundary Condition

During operating ESP, negative high voltage was applied to the corona-discharge. In these cases negative space charges represented in the inter electrode space and negative ions moved toward collecting electrode in ESP when there was not back corona. In the corona space, electric potential field must satisfy Poisson equation and the current continuity equation:

$$\nabla \cdot \vec{E} = -\nabla^2 \varphi = \frac{\rho}{\varepsilon_0} \tag{3}$$

$$\nabla \cdot \vec{j} = 0 \tag{4}$$

$$\vec{j} = -\rho k(\nabla \varphi) = \rho k \vec{E} \tag{5}$$

Where φ was electric potential, V, ρ was charge density, $C \cdot m^{-3}$, j was current density, $A \cdot m^{-2}$, k was ionic mobility, $m^2 \cdot s^{-1} \cdot V^{-1}$; ε_0 was dielectric constant of vacuum,$8.85 \times 10^{-12} C \cdot V^{-1} \cdot m^{-1}$; E was field strength vector , $V \cdot m^{-1}$.

Poisson equation (3) represented the relationship between electric potential and space charges. Equation (4) illustrated the conservation and equation (5) represented ohm's law. The boundary conditions of the equations were:

$$\varphi\big|_{s_1} = \pm V \qquad \varphi\big|_{s_2} = 0 \qquad -\nabla\varphi\big|_{s_3} = E_0$$

Where S_1 was the surface of electrical conductor, S_2 was the surface of earthing conductor, S_3 was the surface of corona zone.

According to Kapston hypothesis:

$$\varphi\big|_{s_4} = 0 \qquad \varphi\big|_{s_5} = V_0 \qquad \rho\big|_{s_5} = \rho_0$$

where S_4 was the surface of the collecting plates, S_5 was the surface of the discharge electrodes. The numerical analysis concerned with the electric field strength and electric potential through calculating equation (3) and equation (4). The electric field strength of corona zone and outside corona zone were used to estimate the performance of the electrode configuration in ESP.

3.2 Validation of the Calculation Model

After eliminating the influence of boundary condition, the electric field of a pipe precipitator was axial symmetry, and the electric potential equation could be predigested to one-dimensional. So the electric potential and electric field strength could be got by calculation. The dependability of the finite element was testified by contrasting the results of calculation and numerical analysis.

For the pipe precipitator, the radius of electric discharge was 0.14 cm, the radius of pipe was 10 cm. The geometric model was listed in Fig. 6. At indoor condition, if 1.2×10^{-6} A/cm was wanted ,how to solve the problem of distribution of electric potential and electric field strength.

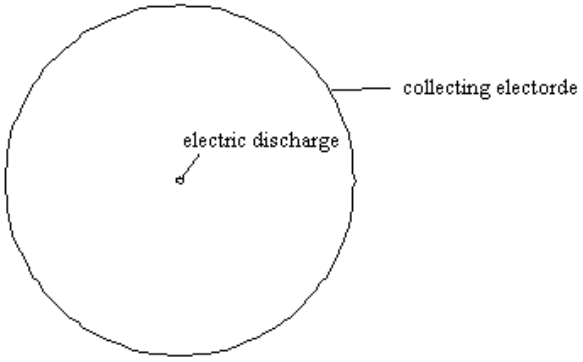

Fig. 6 Geometric model of calculating

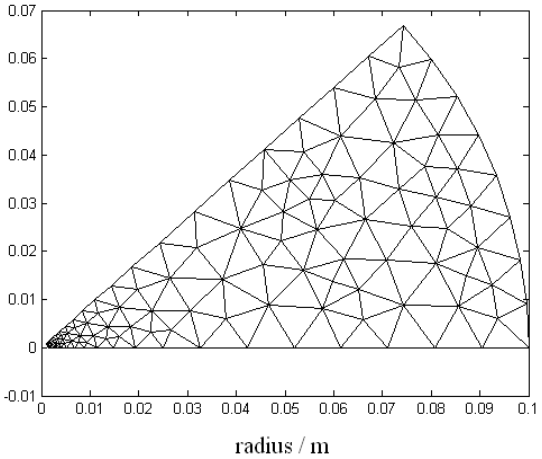

Fig. 7 Delaunay triangulation of a part of pipe precipitator

Delaunay triangle grid was used to dissert part of geometric model. The grid was shown in Fig.7

The distributions of the electric potential and electric field strength by numerical analysis were shown in Fig.8. The results of calculation and numerical analysis were denoted in Cartesian coordinate in Fig.9-Fig.10.

The max deviation of electric potential between calculation and numerical analysis was less than 5%. So the finite element was feasible to calculate the distribution of electric potential and electric field strength.

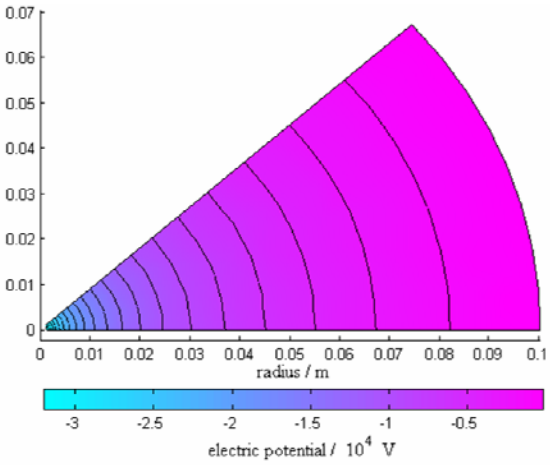

(a) Distribution of electric potential

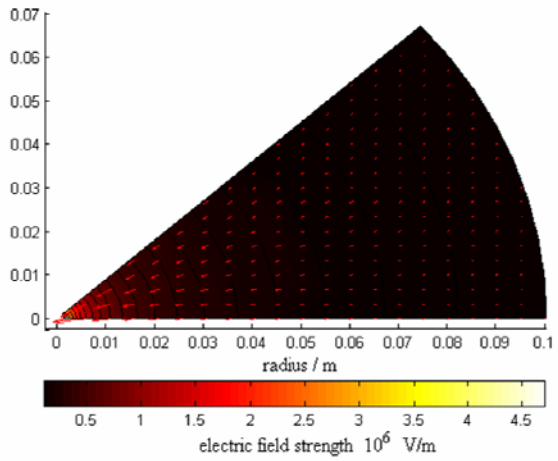

(b) Distribution of electric field strength

Fig. 8 Distribution of electric potential and electric field strength of calculating zone

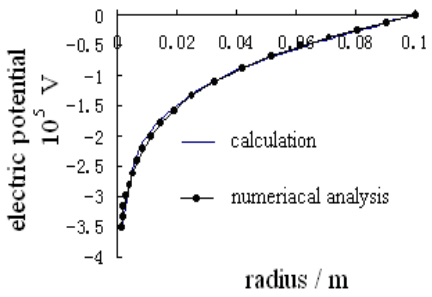

Fig. 9 Results of electric potential analytic solution VS. numerical analysis

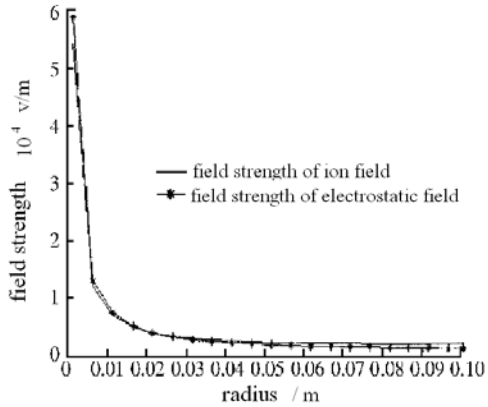

Fig. 10 Calculating results of electric field strength with/no space charges

4 THE APPLICATION OF FINITE ELEMENT METHOD

4.1 Geometric Model and Grid

The method selected the two-dimension face of the discharge electrode and collecting plate as calculated zone, and used discharge electrode V15 and collecting plate ZT24, with plate spacing of 400 mm. The size of geometric model established by the experiment model was shown in Fig. 11. The Delaunay triangulation grid of the calculation zone was shown in Fig. 12.

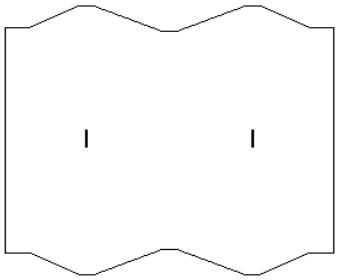

Fig. 11 Geometry graph models

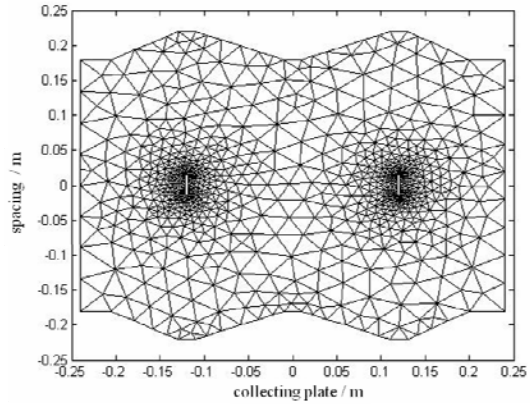

Fig. 12 Gridding of calculating zone

4.2 Results

The distribution of the electric potential and electric strength were shown in Figs. 13 and 14.

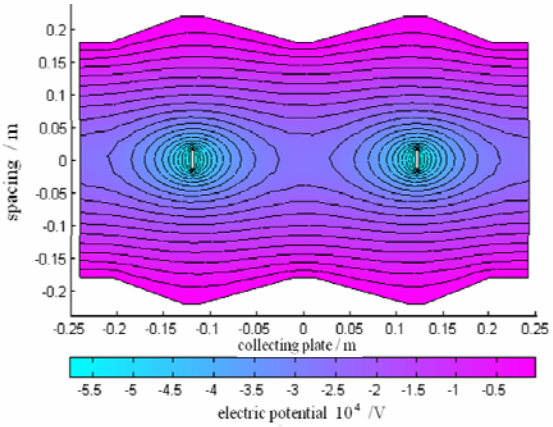

(a) Distribution of electric potential of the whole zone

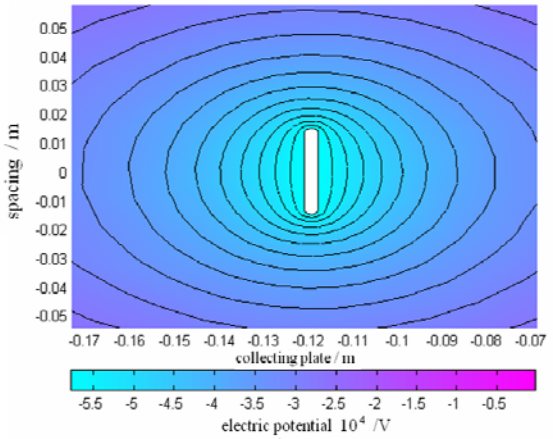

(b) Distribution of electric potential near electrode discharge

Fig. 13 Distribution of the electric potential

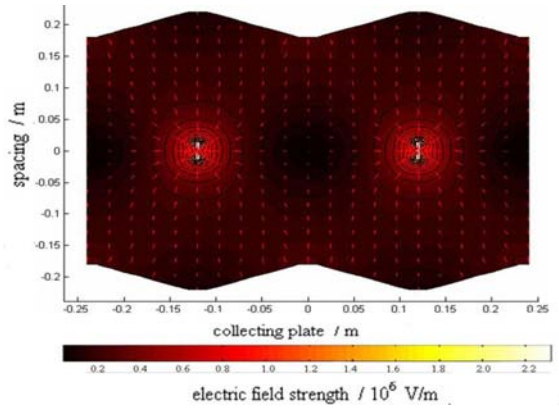

(a) Distribution of electric field strength of the whole zone

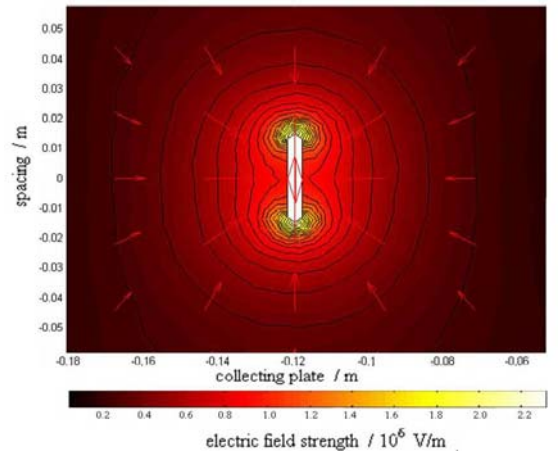

(b) Distribution of electric field strength near discharge electrode

Fig. 14 Distribution of the electric field strength

4.3 Results Analysis of Numerical Analysis and Experiments

4.3.1 The influence of electric strength of corona zone on corona current

In mechanism, the process of electron snowslip was dominated by the ionization electric potential of the gas and the electric strength of corona zone. As to the experiments, the process of electron snowslip was dominated by the electric strength of corona zone. The results of the value of electric strength of corona zone calculated by the finite element were shown in Table 2. From Table 2, it could be seen that on the condition of any plate spacing, the value of electric strength of corona zone of V15 was bigger than V0. Compare with the average of corona current density in the Table 1, it has been shown that the smaller of the curvature radius was, the bigger the corona current was.

Table 2 Distribution of electric field of corona zone combining V0, V15 and ZT24 Unit: 10^5 V/m

Condition:	E_{max}		
$\overline{E}$ =3.15 kV/cm	Spacing: 350 mm	Spacing: 400 mm	Spacing: 450 mm
V0	4.834	4.821	4.810
V15	19.73	23.08	19.40

4.3.2 The influence of electric strength of outside corona zone to corona current

When the curvature radius of corona discharge was constant, the corona current was the main factor to the electric strength of outside corona zone. As the density of outside corona zone raise, the density of line current increased. To the electric field of configuration in the experiments, the average electric strength near collecting plate were shown in Table 3 with the finite element where V15,V25,V40 as corona discharge, ZT24 as collecting plate. Compare with Table 1 and Table 3, it could be seen that when the plates spacing was constant, as the electric strength of outside corona zone enhanced, the average current on the collecting plate increased.

Table 3 Average electric field strength near collecting plate calculated by finite element method Unit: 10^5 V/m

Condition:	$\bar{E}$		
Table=3.15 kV/cm	Spacing: 350 mm	Spacing: 400 mm	Spacing: 450 mm
V15	4.286	3.788	3.602
V25	4.388	4.232	4.134
V40	4.523	4.181	3.888

5 CONCLUSIONS

[1] The experiment results showed that when RS electrodes matched collecting plates C480 and V15,V25,V40 electrodes matched collecting plates ZT24, the distribution of current density on collecting plate was the best with the plate spacing of 400 mm. Meanwhile, it showed that the corona power was the biggest and parameters were better at 400 mm, when the RS discharge matched collecting plate ZT24. The experiment results provide some reference value for the design of ESP.

[2] The paper adopted the finite element method, calculating the electric potential and electric strength on the condition that V serial matched collecting plate ZT24 at plate spacing of 400 mm by building and solving the mathematics model of corona field. Combing the experiment results, we analyzed the effect of electric field strength on corona current. It could be seen that the bigger electric field strength of corona zone was, the bigger current density on collecting plate was. The calculation results tally well with experiment results.

REFERENCES

1. YANG Jinji. Gas discharge [M]. Beijing: Science Press, 1981 (in Chinese).
2. WU Yan. Current research status of the application of pulsed electrostatic technology [J]. Journal of Zhongyuan Institute of Technology, 2003, 14(8): 10-14 (in Chinese).
3. ZHAO Zhibin, WU Yan, et al. Particle charge in pulse corona discharge process [J]. Journal of Environmental Science, 1999, 19(2): 113-119 (in Chinese).
4. FITCH R A, DRUMMOND J E. Enhanced charging of fine particle by electrons in pulse energized electrical precipitator [J]. IEE Proceeding (Part A) , 1987, 134(1): 37-44.
5. WHITE H J. Industrial electrostatic precipitator [M]. Beijing: Metallurgical Industry Press, 1984 (in Chinese).
6. OGLESBY S. Electrostatic Precipitation [M]. Beijing: China Water Power Press, 1983 (in Chinese).
7. COOPERMAN P. A theory for space-charge-limited currents with application to electrical precipitation[J]. AIEE Trans, 1960, 79(47): 47-50.
8. DANG Xiaoqing, et al. Experiment study on the optimum electrode configuration for three-electrode electrostatic precipitators [J]. J of Xi'an Univ of Arch & Tech, 1996, 28 (2): 152-156 (in Chinese).
9. TASSICKER O J. Boundary probe for measurement of current density and electric filed strength with special reference to ionized gases [J]. Proc IEE, 1974, 121(3): 213-220.
10. DANG Xiaoqing, YANG Chunfang, et al. Experiment on current density distribution on plate of different combinations of discharge electrodes with collecting plates [J]. Heavy Machinery, 2005(2): 32-35 (in Chinese).